Journal of Controlled Release 170 (2013) 51–63

Contents lists available at SciVerse ScienceDirect

Journal of Controlled Release

journal homepage: www.elsevier.com/locate/jconrel

GENE DELIVERY

Topical delivery of anti-TNFα siRNA and capsaicin *via* novel lipid-polymer hybrid nanoparticles efficiently inhibits skin inflammation *in vivo*

Pinaki R. Desai [a,1], Srujan Marepally [a,c,1], Apurva R. Patel [a], Chandrashekhar Voshavar [b,c], Arabinda Chaudhuri [c], Mandip Singh [a,*]

[a] College of Pharmacy & Pharmaceutical Sciences, Florida A&M University, Tallahassee, 32307, USA
[b] Eugene Applebaum College of Pharmacy & Health Sciences, Wayne State University, Detroit, 48201, USA
[c] Division of Lipid Science and Technology, Indian Institute of Chemical Technology, Hyderabad 500 007, India

ARTICLE INFO

Article history:
Received 25 November 2012
Accepted 25 April 2013
Available online 3 May 2013

Keywords:
Gene therapy
Percutaneous delivery
siRNA
Hybrid nanoparticles
Skin inflammation
Psoriasis like mouse model

ABSTRACT

The barrier properties of the skin pose a significant but not insurmountable obstacle for development of new effective anti-inflammatory therapies. The objective of this study was to design and evaluate therapeutic efficacy of anti-nociception agent Capsaicin (Cap) and anti-TNFα siRNA (siTNFα) encapsulated cyclic cationic head lipid-polymer hybrid nanocarriers (CyLiPns) against chronic skin inflammatory diseases. Physico-chemical characterizations including hydrodynamic size, surface potential and entrapment efficacies of CyLiPns were found to be 163 ± 9 nm, 35.14 ± 8.23 mV and 92% for Cap, respectively. *In vitro* skin distribution studies revealed that CyLiPns could effectively deliver FITC-siRNA up to 360 μm skin depth. Further, enhanced ($p < 0.001$) Cap permeation from CyLiPns was observed compared to Capsaicin-Solution and Capzasin-HP. Therapeutic efficacies of CyLiPns were assessed using imiquamod-induced psoriatic plaque like model. CyLiPns carrying both Cap and siTNFα showed significant reduced expression of TNFα, NF-κB, IL-17, IL-23 and Ki-67 genes compared to either drugs alone ($p < 0.05$) and were in close comparison with Topgraf®. Collectively these findings support our notion that novel cationic lipid-polymer hybrid nanoparticles can efficiently carry siTNFα and Cap into deeper dermal milieu and Cap with a combination of siTNFα shows synergism in treating skin inflammation.

1. Introduction

The recent development of antibody-based therapeutics that target components of signaling pathways has revolutionized the treatment of chronic inflammatory skin diseases such as psoriasis, atopic dermatitis, eczema [1–3]. However, there are few limiting factors with this therapy such as higher cost and limited targeting ability [4,5]. Small interfering RNA (siRNA)-mediated knockdown of pro-inflammatory cytokines at the messenger RNA (mRNA) level (termed RNA interference), offers an alternative therapeutic strategy to overcome chronic inflammatory conditions. In this process, double-stranded RNAs are cleaved by the cellular nuclease Dicer into short 21–22 mer fragments referred to as siRNA, which enter a ribonuclear protein complex termed as the RNA-induced silencing complex. Guided by the antisense strand of the siRNA, this complex mediates a specific degradation of the corresponding mRNA [6]. In fact, targeted gene suppression by antisense DNA and siRNA has shown promising preclinical results and therefore it is currently in the clinical trials for a variety of diseases, including many forms of cancer (*e.g.*, melanoma, neuroblastoma, and pancreatic adenocarcinoma), genetic disorders and macular degeneration [7].

Transdermal application is a very attractive method of delivering therapeutic agents for treating skin disorders given the easy accessibility of skin and the reduced risk of systemic side effects [8]. However, transdermal permeation of macromolecules such as oligonucleotides or proteins has remained a major technological challenge as the primary barrier of skin, stratum corneum (SC), which limits the delivery of most therapeutic payloads into the deeper layers [9,10] due to its complex barrier properties. Several attempts including use of permeation enhancers, ionotophoresis, electroporation and acoustic methods [11–14] have been developed to deliver sufficient amount of therapeutic agent into the deeper dermal milieu. However, their use is restricted

Abbreviations: Cap, Capsaicin; C-CyLiPn, Cap encapsulated CyLiPn; CGRP, Calcitonin gene related peptide; CLSM, Confocal laser scanning microscopy; CS-CyLiPn, Cap + siTNFα incorporated CyLiPn; CyLiPn, Lipid-polymer nanocarriers; FACS, Fluorescence-activated cells sorter; IHC, Immunohistochemistry; IMQ, Imiquimod; LF, Lipofectamine™ RNAiMAX; PASI, Psoriasis Area and Severity Index; PLGA, Poly(lactic-*co*-glycolic acid); Recv Comp, Receiver compartment; RT-PCR, Real time-PCR; SC + Epi, Stratum corneum + epidermis; SC, Stratum corneum; S-CyLiPn, siTNFα incorporated CyLiPn; siFITC, FITC-conjugated siRNA; siFITC-CyLiPn, siFITC incorporated CyLiPn; siRNA, Small Interfering RNA; siTNFα, siRNA against TNFα.

* Corresponding author at: College of Pharmacy and Pharmaceutical Sciences, Florida A&M University, Tallahassee, FL 32307, USA. Tel.: +1 850 561 2790; fax: +1 850 599 3347.
E-mail address: mandip.sachdeva@gmail.com (M. Singh).
[1] These authors contributed equally.

0168-3659/$ – see front matter © 2013 Elsevier B.V. All rights reserved.
http://dx.doi.org/10.1016/j.jconrel.2013.04.021

due to local tolerance concerns and difficulties in therapeutic feasibility. Use of nanoparticle has shown great potential as novel drug delivery systems [15,16]. Moreover, it offers the advantage of delivering multi-therapeutic agents simultaneously [17–19].

Nanoparticulate delivery systems such as liposomes, polymeric nanoparticles, solid lipid nanoparticles, are well studied for the percutaneous delivery [20]. However, their application is restricted in delivering hydrophilic macromolecules such as nucleic acids, proteins and hydrophobic drugs simultaneously. To overcome this limitation, in the present study we have designed and developed a novel biodegradable lipid-polymer hybrid nanoparticle system (CyLiPn) containing cationic amphiphiles with cyclic pyrrolidinium head group [21], and poly(D,L-lactic-*co*-glycolic acid) (PLGA) [22]. The distinct advantages associated with the use of cationic transfection lipids include their: (a) ease in handling and preparation techniques; (b) ability to inject large lipid:nucleic acid complexes; and (c) low immunogenic response [23]. Further, cyclic pyrrolidinium-based cationic lipids are efficient in delivering nucleic acids under systemic settings [24]. Structural resemblance of the lipid with a well known skin permeating agent azone and its analogs 6-aminohexanoates prompted us to use it for topical application. CyLiPn can be easily formed with a negatively charged hydrophobic PLGA core and a positively charged cationic lipid shell in an aqueous solution by self-assembly process (Fig. 1). Hydrophobic drugs can be incorporated into the core during the self-assembly process. The cationic shell of the resulting drug-loaded nanoparticles can be used to incorporate siRNA.

Co-delivery of nucleic acids and drugs has been proposed to achieve the synergistic effect of drug and gene therapies [25–27]. Further, inflammation is a common characteristic of the most prevalent skin disorders in dermatology including psoriasis and dermatitis. Therefore in the present study, co-delivery of drug and siRNA-based therapy for inflammation was selected. Capsaicin (Cap) exhibits an anti-inflammatory property by the inhibiting PGE_2 and nitric oxide production in peritoneal macrophages [28]. Further, Cap stimulates the release of vasoactive neuropeptides such as substance P and calcitonin gene related peptide (CGRP). Tumor necrosis factor-α (TNFα), a pro-inflammatory cytokine, is one of the major contributors in the complex biology of inflammation. There has been a tremendous interest in neutralizing TNF for therapeutic application in a variety of autoimmune diseases including psoriasis, rheumatoid arthritis, inflammatory bowel disease and psoriatic arthritis [29–31].

The main objective of the study was to formulate therapeutically effective CyLiPn comprising of an anti-inflammatory drug Cap and siRNA against TNF-α (siTNFα) to treat difficult skin inflammatory conditions *in vivo*. Hence to achieve this primary goal, the specific aims of this study were: (i) to prepare and characterize CyLiPn formulations containing Cap and/or siRNA (siTNFα), (ii) to examine the cellular uptake and skin distribution of FITC-labeled siRNA (siFITC) incorporated into CyLiPn *in vitro*, (iii) to evaluate the *in vitro* skin retention and permeation of C-CyLiPn, (iv) to therapeutically assess the efficacy of CyLiPn to treat inflammation in imiquimod (IMQ)-induced psoriatic plaque like mouse model using scoring, histological examination, and immunohistochemistry (IHC) — TNFα, NF-κB; Western blotting — TNFα, Ki-67, NF-κB, IL-17, IL-23; and Real time-PCR (RT-PCR) — TNFα, NF-κB.

2. Materials and methods

2.1. Materials

Polyoxyethylene-20 oleyl ether (Volpo-20) was a kind gift from Croda Inc. (Edison, NJ, USA). Phosphate buffer saline sachets (PBS, pH 7.4), DEPC (diethylpyrocarbonate)-treated and sterile filtered water, Tris acetate-EDTA (TAE) buffer, ethidium bromide, PEG_{400} and trifluoroacetic acid were purchased from Sigma-Aldrich Co. (St. Louis, MO, USA). HPLC grade of acetonitrile, water and ethanol were purchased from Sigma-Aldrich Co. (St. Louis, MO, USA). Capsaicin was purchased from EMD Millipore Corporation (Billerica, MA, USA). PLGA was purchased from PURAC Biomaterials (Lincolnshire, IL, USA). 1,2-dioleoyl-*sn*-glycero-3-phosphocholine (DOPC), 1,2-distearoyl-*sn*-glycero-3-phosphoethanolamine-N-[amino(poly-ethylene glycol)-2000] (ammonium salt) ($DSPE\text{-}PEG_{2000}$) were purchased from Avanti Polar Lipids, Inc. (Alabaster, AL, USA). Imiquimod (IMQ) was purchased from Enzo Life Sciences, Inc. (Farmingdale, NY, USA). Topgraf® was purchased from GlaxoSmithKline Pharmaceuticals Limited (Thane, MH, India). Lipofectamine™ RNAiMAX transfection reagent was purchased from Life Technologies Corporation (Grand Island, NY, USA). BCA protein assay reagent kit was procured from Pierce Biotechnology, Inc. (Rockford, IL, USA). RIPA lysis and extraction buffer was purchased from G-Biosciences (Maryland Heights, MO, USA). RNeasy kit, RT^2 first strand kit and RT^2 SYBR Green ROX qPCR Mastermix were purchased from QIAGEN Inc. (Valencia, CA, USA). siRNA against TNFα (siTNFα), FITC-labeled siRNA (siFITC), antibodies against TNFα, NF-κB, Ki-67, IL-17, IL-23, β-actin, secondary HRP antibody, ABC staining immunohistochemistry (IHC) kit and primers against TNFα, NF-κB and β-actin were purchased from Santa Cruz Biotechnology, Inc. (Santa Cruz, CA, USA). HEK-293 cells were grown in DMEM (Dulbecco's modified Eagle's medium) medium

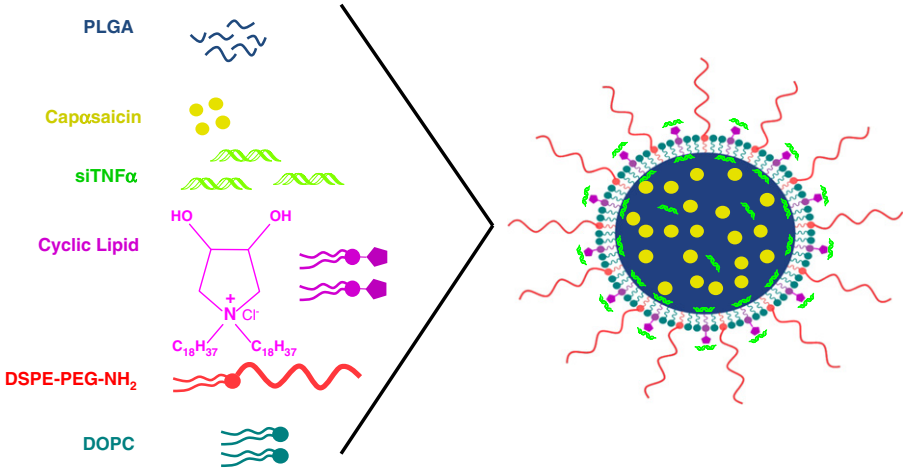

Fig. 1. Schematic illustration shows the formulation of CyLiPn. The CyLiPn comprises a hydrophobic PLGA core, a hydrophilic PEG shell and a lipid monolayer consisting of 1,2-dioleoyl-sn-glycero-3-phosphocholine (DOPC) and a new cationic cyclic-head lipid at the interface of the hydrophobic core and hydrophilic shell.

(Sigma-Aldrich Corporation, St. Louis, MO, USA) supplemented with 10% FBS (fetal bovine serum) and antibiotic antimycotic solution of penicillin (5000 U/ml), streptomycin (0.1 mg/ml) and neomycin (0.2 mg/ml). The cells were maintained at 37 °C under 5% CO_2. All other chemicals used in this research were either of analytical grade or tissue culture grade.

2.2. Animals

CD®(SD) hrBi hairless rats (350–400 g; male; Charles River Laboratories, Wilmington, MA, USA) and C57BL/6 mice (6 weeks old; male; Charles River Laboratories, Wilmington, MA, USA) were grouped and housed (n = 6 per cage) in cages with bedding. The animals were kept under controlled conditions of 12:12 h light:dark cycle, 22 ± 2 °C and 50 ± 15% RH. The mice were fed (Harlan Teklad) and could drink water *ad libitum*. The animals were housed at Florida A&M University in accordance with the standards of the Guide for the Care and Use of Laboratory Animals and the Association for Assessment and Accreditation of Laboratory Animal Care (AAALAC). The animals were acclimatized to laboratory conditions for one week prior to experiments. All the animal protocols followed were approved by the Animal Care and Use Committee, Florida A&M University, FL, USA.

2.3. Preparation of formulations

2.3.1. Preparation of lipid-polymer nanocarriers (CyLiPn)

The cationic lipid with cyclic 3,4-dihydroxy-pyrrolidinium headgroup was synthesized by dehydrative coupling of the octadecylamine to L(+)-tartaric acid in refluxing xylene so that water formed during the reaction could be separated by azeotropic distillation in a Dean–Stark apparatus. The resulting N-n-alkyl-3,4-dihydroxy-2,5-dioxo pyrrolidine (cyclic imide interemedite I), upon reduction with sodium borohydride/iodine, afforded the corresponding tertiary amine intermediate II the immediate precursor of the target lipids. Intermediate II, upon quaternization with hydrophobic octadecyl bromide in 3:1 (v/v) ethylacetate/acetonitrile followed by chloride ion exchange on Amberlyst-A26 resin, afforded the target lipid [24]. Then nanoparticles were prepared by a previously reported double emulsion solvent evaporation method [32] with few minor changes. CyLiPns were prepared *via* self-assembly of PLGA; DOPC, cyclic cationic lipid and DSPE — PEG_{2000} through a single-step nano-precipitation method. Briefly, inner polymeric core was prepared by dissolving 5 mg of PLGA in acetonitrile. Cyclic head cationic lipid/DOPC/DSPE — PEG_{2000} (4.0/4.5/1.5, molar ratio) with a weight ratio of 15% to the PLGA polymer was dissolved in 4% ethanol aqueous solution. The lipidic solution was heated to 65 °C under gentle stirring to ensure that all the lipids were in the liquid phase. Once the temperature was decreased to 30–35 °C, 300 μl of 10 μM siRNA solution was added drop-wise with gentle stirring. This solution was stirred for 10 min. The PLGA solution was then added into the preheated lipid solution drop-wise under gentle stirring. After the addition, organic solvent was allowed to evaporate for 4–12 h under stirring leading to nano-precipitation [33]. Finally, the remaining organic solvent was removed by rotary evaporation.

The Blank-CyLiPn was prepared using the same procedure as explained above without addition of drug or siRNA. To prepare Cap encapsulated nanoparticles (C-CyLiPn), 2.5 mg of Cap was dissolved in organic phase containing PLGA and the remaining procedure is the same, however siRNA was not added. While FITC-conjugated siRNA (siFITC) incorporated nanoparticles (siFITC-CyLiPn) were prepared by adding only siFITC in the lipidic aqueous solution. In a similar way, siTNFα incorporated CyLiPn (S-CyLiPn) was also prepared by adding siTNFα into the lipidic aqueous solution. Finally, a combination of Cap and siTNFα encapsulated CyLiPn (CS-CyLiPn) was prepared by adding Cap in an organic phase and siTNFα in an aqueous phase.

2.3.2. Preparation of solutions

The siFITC-Solution was prepared by simply dissolving fluorescently labeled siRNA (siFITC) into DEPC-treated water. In a similar way siTNFα-Solution was prepared by adding siTNFα in DEPC-treated water. Further, Cap containing solution (C-Solution) was prepared by dissolving a known amount of Cap in 10% v/v ethanol in polyethylene glycol (PEG_{400}). In addition to CyLiPn formulations, Cap + siTNFα solution (CS-Solution) was formed in 10% v/v ethanol and in polyethylene glycol (PEG_{400}).

2.4. Physicochemical characterization of nanoparticles

The particle size and zeta potential of Blank-CyLiPn, C-CyLiPn, S-CyLiPn and CS-CyLiPn were measured using Nicomp 380 ZLS as explained previously [16–19]. The assay was performed by dissolving 100 μl of CyLiPn in 900 μl of ethanol. The samples were then centrifuged at 13,000 rpm for 15 min and 100 μl of supernatant were tested to determine the total amount (bound and unbound) of the Cap and siTNFα present in C-CyLiPn, S-CyLiPn and CS-CyLiPn formulations [17]. The Cap content was determined by high-performance liquid chromatography (HPLC). While the siTNFα content was measured by the Quant-iT™ RiboGreen® RNA kit (Molecular Probes, Inc., Eugene, OR, USA) according to the manufacturer's instructions and the fluorescence was measured using Tecan® 200 PRO microplate reader (Männedorf, Switzerland). The entrapment efficiency of Cap in the C-CyLiPn and CS-CyLiPn was determined by using vivaspin columns as explained earlier [16]. Each sample was analyzed in triplicate.

2.5. Gel retardation and siRNA integrity assay

The incorporation of siTNFα in S-CyLiPn and CS-CyLiPn was determined by 2% agarose (low melting point) gel electrophoresis. For comparison, siTNFα solution was used. The siRNA was extracted from the CyLiPn as described in Section 2.4 in assay method and loaded with the other test samples to test the integrity. Twenty microliters of the sample containing 1:6 dilution of loading dye (Pierce Biotechnology, Inc., Rockford, IL, USA) was added to each well and electrophoresis was carried out at a constant voltage of 100 V, for 30 min in TAE buffer containing 0.5 μg/ml ethidium bromide. The siRNA bands were then visualized under UV transilluminator (Gel Doc™ XR + System, Bio-Rad Laboratories, Inc., Hercules, CA, USA) at a wavelength of 365 nm [34].

2.6. Cytotoxicity of nanoparticles

The cell viability in the different treatment groups and control group was evaluated by MTT method. HEK-293 cells were seeded into 24-well plates at a density of 1×10^5 cells/well in 0.5 ml of DMEM complete growth medium and incubated for 24 h to allow for cell adherence. The growth media was not changed prior to addition of the test formulas in order to get least variation in the results. The cells were then treated with different volumes of Blank-CyLiPn and CS-CyLiPn formulation starting from 1 μl to 40 μl. After 24, 48 and 72 h, 20 μl of 5 mg/ml MTT [3-(4,5-dimethylthiazol-2-yl)-2,5-diphenyltetrazolium bromide] (EMD Millipore Corporation, Billerica, MA, USA) solution was added to each well and cells were incubated for 4 h at 37 °C [34]. Then, the MTT containing medium was aspirated and the formazan crystals formed by the living cells were dissolved in 150 μl DMSO. The absorbance was measured spectrophotometrically in Tecan® 200 PRO microplate reader at 570 nm. Untreated cells were taken as control with 100% viability and cells without the addition of MTT were used as blank to calibrate the spectrophotometer to zero absorbance. The relative cell viability (%) compared to control cells was calculated by $[abs]_{sample} / [abs]_{control} \times 100$.

2.7. Cellular uptake of CyLiPn

HEK-293 cells were seeded in a 24-well plate at a density of 10^5 cells/well and incubated in 0.5 ml of complete growth medium for 24 h to allow cell adherence. The medium was removed and the cells were washed twice with Dulbecco phosphate buffered saline (Cellgro®, Corning Manassas, VA, USA) and replaced with 0.5 ml of Opti-MEM® reduced serum medium (Gibco®, Life Technologies Corporation, Grand Island, NY, USA). Then, siFITC-Solution, LF-siFITC (Lipofectamine™ RNAiMAX) complexes and 10 μl (optimized volume) of siFITC-CyLiPn were added to 24-well plates. After 12 h of culture, the transfection medium was removed and cells were washed. Then the intercellular siFITC uptake and localization was imaged using inverted microscope Olympus BX40 microscope equipped with computer-controlled digital camera (DP71, Olympus Center Valley, PA, USA). Further, the intercellular fluorescence was determined using fluorescence-activated cells sorter (FACS)Calibur flow cytometer (BD Biosciences, Franklin Lakes, NJ, USA).

2.8. In vitro percutaneous permeation

2.8.1. Preparation of skin

For skin collection, CD®(SD) hrBi hairless rats were sacrificed by an overdose of halothane anesthesia. The hairs were clipped off by using hair clippers. Extra precautions were taken while performing this procedure in order to avoid any damage to the skin. The skin from the dorsal surface was excised, and then adherent subcutaneous fat and connective tissues were removed carefully. The storage conditions were previously optimized by our laboratory where the effect of different storage conditions on the permeation of melatonin and nimesulide by using cryoprotecting agent (CPA) were studied. We have observed that the incubation of skin in aqueous glycerol (a well-known CPA) followed by freezing at −22 °C can maintain the viability for longer periods [35]. In addition, the report on guidelines on processing and clinical use of skin allografts showed that skin storage at −80 °C can provide long term storage with the use of CPA [36]. Therefore, in the present study the skin was stored in 10% w/w glycerol in saline at −80 °C and used within 1 week. Prior to use, the skin was rinsed in PBS (pH 7.4) for 30 min to remove excess of glycerol. Further, the integrity of the skin was evaluated by comparing a resistance of fresh skin and thawed skin before starting the skin permeation experiment. If any difference between the resistance of fresh skin and thawed skin was measured then the skin was discarded.

2.8.2. In vitro permeation of formulations

The skin was mounted on vertical Franz diffusion cells (PermeGear Inc., Riegelsville, PA, USA) with the epidermis facing the donor compartment. One hundred microliters of the test formulations were applied on the diffusion surface of the skin in the donor compartment. The receiver compartment (Recv Comp) was filled with 5 ± 0.5 ml PBS (pH 7.4) containing 0.1% volpo-20, stirred at 300 rpm and maintained at 32 ± 0.5 °C using a circulating water bath. Skin permeation studies were performed for 24 h under unocclusive conditions. To perform the skin collection after 24 h, the donor cell was removed and the excess formulation was removed from the surface of the skin using a cotton swab. The skin was then washed with 50% v/v ethanol and blotted dry with lint-free absorbent wipes. The entire dosing area (0.636 cm^2) was collected with a biopsy punch. The collected skin was then used for further studies.

2.9. Skin imaging studies

The imaging was performed using confocal laser scanning microscopy (CLSM) to study the skin distribution of the FITC-labeled siRNA incorporated CyLiPn and siFITC-Solution. The amount of siFITC applied was maintained samely for both the applications. In this study, rat skin was selected as a model skin and the *in vitro* permeation study was performed as explained in the 2.8.2 section. The skin imaging was performed as described by Shah et al. [17]. Briefly, to visualize skin-associated fluorescence, the full thickness skin sections and lateral skin sections were collected up to 360 μm using cryotome (Shandon, England). The skin sections were visualized with CLSM (Leica Microsystems Inc., Buffalo Grove, IL, USA) using 10× objective and throughout the study period instrument settings were kept constant. Finally, the collected images were analyzed using Digital image software (Museum of Science, Boston, MA, USA) for the skin-associated fluorescence.

2.10. Skin permeation and retention of capsaicin

The *in vitro* rat skin permeation was performed for C-Solution, marketed Capzasin-HP Cream (Capsaicin Cream 0.1%, Chattem Inc., Chattanooga, TN, USA) and C-CyLiPn [15]. After 24 h of skin permeation, the receiver fluid was collected and centrifuged at 13,000 rpm for 15 min and analyzed for drug content using HPLC.

2.10.1. Capsaicin skin extraction

Cap formulation-exposed skin was collected after 24 h. Epidermis containing SC (SC + Epi) was then separated from the dermis using sharp forceps. Then collected layers were cut into small pieces. Two hundred fifty microliters of PBS (pH 7.4) was then added to all the collected skin layers and heated on boiling water bath. After 10 min, all the samples were cooled down to room temperature and then 250 μl of acetonitrile was added. The vials were sonicated in a bath sonicator for 30 s and then vortexed for 2 min. Finally, all the tissue samples were centrifuged at 13,000 rpm for 15 min. The supernatant was collected and the extracts were analyzed for Cap content using HPLC.

2.10.2. HPLC analysis

The HPLC analysis of Cap was performed with minor modifications from a reported method [16]. Briefly, Waters HPLC system was comprised of an auto sampler (model 717 plus), binary pump (model 1525), UV photodiode array detector (model 996). The mobile phase consisting of acetonitrile (70% v/v), water (30% v/v), trifluoroacetic acid (0.1% v/v) was pumped through the Symmetry C18 column (5 μm, 4.6 × 250 mm) at a flow rate of 1.0 ml/min and the eluent was monitored at 280 nm. The Cap stock solution was prepared in acetonitrile and the serial working standard solutions were prepared in mobile phase. All injections were performed at room temperature.

2.11. In vivo imiquimod-induced psoriatic plaque like model

The psoriatic plaque like model was developed as described earlier [18]. Briefly, IMQ suspension was applied topically on the shaved back of C57BL/6 mice. To the inflamed skin area, test formulations were applied topically every day for 5 days. CyLiPn formulations of Cap and siTNFα alone and in combination were tested in comparison with CS-Solution. Topgraf® was used as a positive control.

2.11.1. Scoring severity of skin inflammation

The objective scoring system was developed based on the clinical Psoriasis Area and Severity Index (PASI) to score the severity of inflammation [19]. Erythema, scaling and thickening were scored independently on a scale from 0 to 4: 0, none; 1, slight; 2, moderate; 3, marked; 4, very marked. The scoring was performed every 24 h for 5 days.

2.11.2. Histological analysis

The inflamed skin was collected at the end of experiment and stored in 10% neutral phosphate buffered formalin. Following fixation, samples

were dehydrated and embedded in paraffin. Five micrometer microtome sections of the inflamed skin were then stained with hematoxylin and eosin. The Olympus BX40 light microscope equipped with computer-controlled digital camera was used to visualize the images on the slides.

2.11.3. Immunohistochemistry

IHC study was performed for TNFα and NF-κB [18]. In brief, formalin-fixed, paraffin-embedded skin sections were used for IHC studies according to the protocol specified in the ImmunoCruz™ mouse ABC staining kit. The section slides were washed in xylene and hydrated in different concentrations of alcohol. The slides were incubated with the primary antibody against TNFα and NF-κB separately overnight at 4 °C. Horseradish peroxidase-conjugated secondary antibody was applied to locate the primary antibody. The specimens were stained with DAB chromogen and counterstained with hematoxylin. The presence of brown staining was considered a positive identification for activated TNFα and NF-κB. The inverted microscope Olympus BX40 microscope was used to visualize the images on the slides.

2.11.4. Western blot analysis

The skin tissues were harvested from normal and treated (IMQ, S-CyLiPn, C-CyLiPn, CS-CyLiPn, CS-Solution and Topgraf®) mice and minced into small pieces and homogenized in PBS. The homogenate was centrifuged at 13,000 rpm speed for 10 min to sediment the tissue fragments. The proteins were extracted using RIPA lysis and extraction buffer with protease inhibitor (500 mM phenylmethylsulfonyl fluoride). Protein content was measured using BCA protein assay reagent kit according to the manufacturer's protocol. The protein samples (50 μg) were loaded and subjected to SDS-polycrylamide gel electrophoresis (SDS-PAGE) as previously described [37,38]. The blots were then probed with primary antibodies targeting TNFα, Ki-67, NF-κB, IL-17, IL-23 and β-actin. HRP-conjugated secondary antibodies were then used to label the bound primary antibodies. Chemiluminescent detection of antibody-labeled proteins was done using a SuperSignal West Pico chemiluminescent substrate (Pierce Biotechnology, Inc., Rockford, IL, USA) and exposed to Kodak X-OMAT AR autoradiography film (Eastman Kodak Company, Rochester, NY, USA). The densitometric analysis of the bands was performed using the program Image J v1.33u.

2.11.5. Real-time PCR analysis

Total RNA was extracted from biopsies of the mouse back skin using RNeasy kit and converted to complementary DNA using RT^2 first strand kit and RT^2 SYBR Green ROX qPCR Mastermix as per the manufacturer's instructions. Amplification was performed on an ABI 7300 RT-PCR (Applied Biosystems, Carlsbad, CA, USA) and data analysis was done with a PCR array data analysis software (SABiosciences, Valencia, CA, USA). The mRNA levels of TNFα, NF-κB and β-actin were then calculated. The β-actin was used as a normalization control for gene expression.

2.12. Statistical analysis

Data were expressed as the means and standard deviation (mean ± SD). One-way ANOVA followed by Tukey's multiple comparison test was performed to determine the significance of differences among groups using GraphPad PRISM version 5.0 software (La Jolla, CA, USA). Differences were considered significant at $p < 0.001$ or $p < 0.05$.

3. Results

3.1. Physicochemical characterization of nanoparticles

Blank-CyLiPn had particle sizes in the range of 150–180 nm with mean particle size of 163 ± 9 nm. The CyLiPn showed a narrow size distribution with PI of 0.054 ± 0.02. The zeta potential of the Blank-CyLiPn in double distilled water (pH 6.4) was found to be 35.14 ± 8.23 mV. The encapsulation of the Cap or siTNFα in CyLiPn (C-CyLiPn, S-CyLiPn and CS-CyLiPn) showed less effect on particle size or zeta potential. The detailed summary of the physicochemical properties is summarized in Table 1. The total Cap present in C-CyLiPn and CS-CyLiPn dispersion was found to be 0.82 ± 0.09 mg/ml and 0.79 ± 0.19 mg/ml, respectively. This assay value was used to calculate the percent entrapment and percent dose permeation.

3.2. Gel retardation and siRNA integrity assay

The incorporation of siTNFα into CyLiPn formulations (S-CyLiPn and CS-CyLiPn) leads to complex formation between cationic lipid and anionic siRNA. This can result in the electro-neutralization of the negative charge of the siTNFα and therefore siTNFα might be unable to migrate under the influence of the electric field during the gel electrophoresis. To confirm the incorporation of the siTNFα into CyLiPn formulations, a gel retardation assay was performed. As shown in Fig. 2, complete incorporation of the siTNFα (without the presence of a free siRNA band) was observed for S-CyLiPn (lane ii) and CS-CyLiPn (lane iv). Further, when siTNFα was loaded in the form of simple aqueous solution, a clear band was observed (lane i). The extracted siTNFα from S-CyLiPn (lane ii) and CS-CyLiPn (lane v), formulations was intact and was able to migrate in the electric field.

3.3. Cytotoxicity of nanoparticles

To estimate the extent of toxicity caused by CyLiPn formulations, MTT colorimetric assay was performed after 24, 48 and 72 h (Fig. 3). The results showed that the toxicity on HEK-293 cells was enhancing with the increasing volume of CyLiPn. The treatment of the cells with Blank-CyLiPn up to 10 μl volumes did not induce obvious cell toxicity even after 72 h. However, cell viability was decreased to 75.85 ± 2.96%, 72.69 ± 2.84% and 63.53 ± 3.52% after the addition of 40 μl of Blank-CyLiPn at 24, 48 and 72 h, respectively. The toxicity of the formulations was not increased significantly by incorporating Cap and siTNFα into CyLiPn. The trend of the toxicity from CS-CyLiPn was observed to be the same. The toxicity from the CS-CyLiPn was increased with increasing volume of the CS-CyLiPn and time of exposure. However in any case, the cell viability after 72 h was not significantly different than those from 24 and 48 h indicating that, the high cell toxicity was due to the higher volume of CyLiPn. These results suggest that the inclusion of the cyclic head cationic lipid can affect the relative cell viability at the higher concentration. For the cellular uptake study, 10 μl was selected as an optimum volume of the CyLiPn. As at this concentration the cell viability was more than 92% even after 72 h. With this toxicity profile, it can be also proposed that the CyLiPn formulation would be safe to use for *in vivo* experiments.

3.4. Cellular uptake study of CyLiPn

The cellular uptake efficiency of siFITC-Solution, LF-siFITC complexes and siFITC-CyLiPn was compared using fluorescence microscopy and FACS. The examination of cultured HEK-293 cells after 12 h of incubation under fluorescent microscope showed that siFITC-CyLiPn had increased intercellular siFITC delivery efficiencies than siFITC-Solution and LF-siFITC (Fig. 4). HEK-293 cells showed very high uptake of the siFITC from CyLiPn, that is, ~95% of the cells

Table 1
The physicochemical properties of CyLiPn. Data represent mean ± SD (n = 6).

Formulations	Particle size (nm)	Polydispersity	Zeta potential (mV)	Theoretical loading of siRNA	Entrapment efficiency of Cap
SiFITC-CyLiPn	160.82 ± 2.37	0.096 ± 0.002	31.2 ± 3.46	68.26 ± 3.71%	–
C-CyLiPn	164.54 ± 5.13	0.096 ± 0.003	38.1 ± 2.63	–	91.26 ± 4.63%
S-CyLiPn	159.45 ± 3.76	0.084 ± 0.004	30.4 ± 4.57	70.27 ± 4.16%	–
CS-CyLiPn	167.73 ± 8.35	0.102 ± 0.006	30.05 ± 3.26	69.56 ± 3.41%	90.87 ± 6.23%

were siFITC positive. Quantitative cellular uptake of siFITC was estimated using a FACSCalibur flow cytometer, which further confirmed the results observed by fluorescent microscopy (Fig. 5A and B). The maximal siFITC uptake efficiency was obtained in the CyLiPn group, which was significantly higher ($p < 0.05$) than that of the LF-siFITC group (92.28 ± 2.46% *vs.* 74.43 ± 3.51%). However, there was only a small amount of uptake detected in the cells when treated with siFITC-Solution.

3.5. Skin imaging studies

The results from CLSM are summarized in Fig. 6. These results clearly showed that incorporation of siFITC into CyLiPn can enhance the skin permeation of siFITC. Fig. 6A displays the images of the skin sections observed under CLSM after the permeation of the siFITC. CLSM studies demonstrated that the fluorescence from the siFITC-Solution decreased with an increase in skin depth. Intense fluorescence for siFITC-Solution was observed up to 40 μm which was decreased at 80 μm and then diminished at 120 μm. On the other hand, fluorescent signal from CyLiPn formulation was observed deep into the dermal region at a depth of 320 μm with higher intensity. The percent fluorescence intensity, calculated from confocal microscopic images, was found in the range between 0 and 18 (Fig. 6B). First two sections 0–20 and 21–40 μm are both superficial, *i.e.*, both correspond to the skin surface, as concluded from the presence of corneocytes undergoing desquamation. The fluorescence intensity of siFITC from CyLiPn is significantly higher ($p < 0.001$) than that from the solution up to a depth of 280 μm. These results suggest that CyLiPn can deliver siRNA into the skin by breaching the SC barrier.

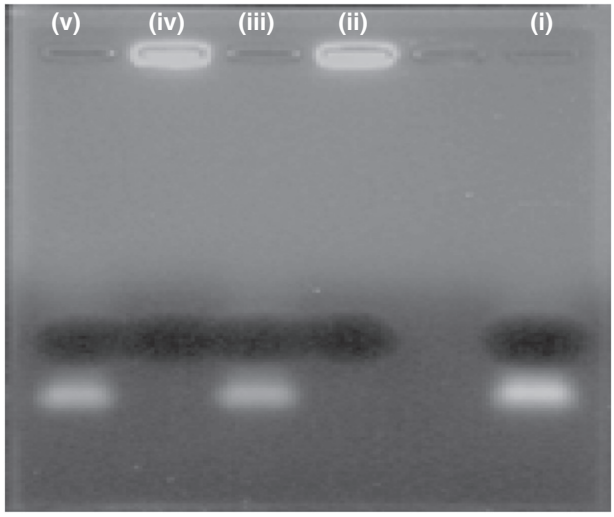

Fig. 2. Gel retardation and siTNFα integrity assay of siTNFα-CyLiPn: lane (i), siTNFα-Solution; lane (ii), S-CyLiPn; lane (iii), extracted siTNFα from S-CyLiPn; lane (iv), CS-CyLiPn; lane (v) extracted siTNFα from CS-CyLiPn.

3.6. Skin permeation and retention of capsaicin

The detection of Cap levels in skin layers and in Recv Comp was determined using HPLC. Fig. 7 shows the effect of CyLiPn formulation on the skin permeation of Cap. The percent of Cap permeated in the SC + Epi, dermis and Recv Comp from C-CyLiPn was 2.43 ± 0.13, 5.21 ± 0.42 and 14.38 ± 0.83%, respectively. The skin permeation of Cap from C-Solution was significantly low compared to C-CyLiPn. Interestingly, the permeated amount of the Cap form CyLiPn was significantly higher than the marketed formulation (Capzasin-HP Cream). C-CyLiPn can deliver 5.8, 2.9 and 4.2 folds more drugs than C-Solution and 3.5, 2.6 and 2.5 folds higher amounts of drug than Capzasin-HP Cream in epidermis, dermis and Recv Comp, respectively.

3.7. In vivo imiquimod-induced psoriatic plaque like model

Induction of psoriatic-like plaques was performed by topical application of IMQ for 5 consecutive days. After 2 or 3 days of IMQ application, the skin started showing signs of erythema and thickening which lead to the observation of the inflammation.

3.7.1. Scoring severity of skin inflammation

The scaling of the mice back skin, a phenomenon typical for psoriatic skin lesions, were observed after topical applications of CyLiPn formulations (C-CyLiPn, S-CyLiPn and CS-CyLiPn); CS-Solution; and Topgraf® (Table 1). The scores of individual mice in every group were consistently very similar within the group resulting in the typically minimal standard deviation. The PASI score for IMQ-control was 4 at the end of the 5th day. However, the PASI score for CS-CyLiPn was decreased to 0 after 5 days of treatment. Overall, compared to individual drug or siRNA treatment, the combination treatment (Cap + siTNFα) showed faster and complete heading at the end of the treatment. On the other hand, the solution containing naked Cap and siTNFα was unable to show the healing at end of the treatment (5th day). For Topgraf®, the PASI score was zero from the 2 days of treatment (Table 2).

3.7.2. Histological analysis

The images from H&E staining of skin tissues from different treatment groups are summarized in Fig. 8. The analysis of H&E stained sections from the IMQ-treated skin showed increased epidermal thickening with elongation of epidermal rete ridges, a disturbed epidermal differentiation and infiltration of leukocytes into both, dermis and epidermis compared to normal skin (Fig. 8, i and ii). Further, the skin from the CS-CyLiPn treatment has very similar characteristics to that of the normal skin (Fig. 8, i and vi). In addition, these results demonstrate that from all tested formulations, CS-CyLiPn formulation can best treat the inflammation caused by IMQ application.

3.7.3. Immunohistochemistry

IHC for TNFα and NF-κB markers was performed on the collected skin sections and the results are represented in Fig. 9. The presence of brown staining was considered a positive identification for activated TNFα

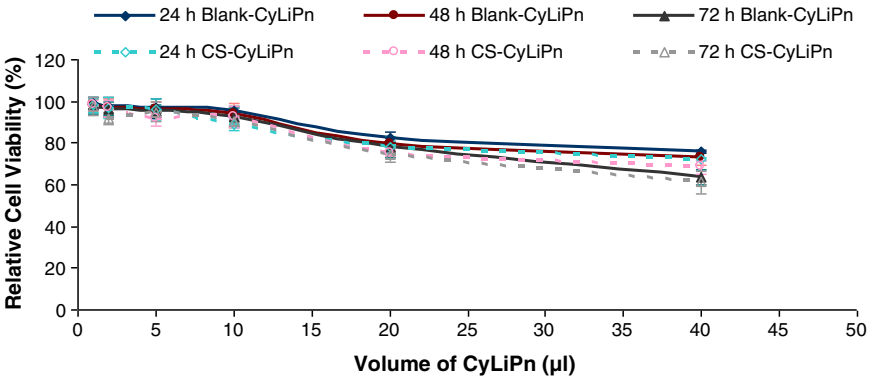

Fig. 3. Relative cell viability of HEK-293 cells on incubation with different volumes of the Blank-CyLiPn and CS-CyLiPn formulations after 24, 48 and 72 h. Data represent mean ± SD (n = 6).

(Fig. 9A) or NF-κB (Fig. 9B). The positive stained cells were quantified and were found in the order of: Normal < CS-CyLiPn < Topgraf® < S-CyLiPn < C-CyLiPn < CS-Solution < IMQ. The results indicate that, the application of siTNFα in a form of CyLiPn (S-CyLiPn and CS-CyLiPn) can knock down the TNFα gene and as a result of that, less expressions of TNFα and subsequently NF-κB was observed.

3.7.4. Western blot analysis

The expression of several inflammatory proteins including TNFα in normal skin tissue lysates was examined. The skin lysates from IMQ and treated mice (CyLiPn formulations — C-CyLiPn, S-CyLiPn and CS-CyLiPn; CS-Solution; and Topgraf®) were analyzed by Western blot using β-actin as a loading control (Fig. 10). The TNFα knockdown was observed for siTNFα treated skin (S-CyLiPn and CS-CyLiPn). Further, for tested proteins (TNFα, Ki-67, NF-κB, IL-17 and IL-23), the increased expression was observed for IMQ-treated skin compared to normal skin. The treatment with positive control (Topgraf®) showed decreased expression of inflammatory proteins (TNFα, Ki-67, NF-κB, IL-17 and IL-23). Results in Fig. 10 further showed that the relative expression of TNFα, Ki-67, NF-κB, IL-17 and IL-23 proteins were decreased in skin tissues from CS-Solution, S-CyLiPn, C-CyLiPn and CS-CyLiPn compared to IMQ-treated skin tissues. Also, a decreased expression of TNFα to 1.77 fold, Ki-67 to 1.53 fold, NF-κB to 1.88 fold, IL-17 to 4.51 fold and IL-23 to 1.06 fold, was observed for CS-CyLiPn compared to CS-Solution. Overall, CS-CyLiPn showed significantly ($p < 0.05$) less expression of inflammatory markers compared to C-CyLiPn, S-CyLiPn and CS-Solution.

3.7.5. Real-time PCR analysis

The relative mRNA levels for TNFα and NF-κB from CyLiPn formulations (C-CyLiPn, S-CyLiPn and CS-CyLiPn); CS-Solution; and Topgraf® are illustrated in Fig. 11. The expression trend for the inflammatory markers was the same as observed for the Western blot analysis. The TNFα and NF-κB mRNA expression was increased for IMQ-treated mouse skin compared to normal mouse skin. However, decreased mRNA levels were observed for the treatments for both the proteins. Further, siTNFα in the form of CyLiPn can deliver biologically active siTNFα to knock down the TNFα gene but when applied in the form of naked siTNFα-Solution, then the biological activity was decreased. Topgraf® and CS-CyLiPn treated skin tissues showed minimum mRNA expressions of both TNFα and NF-κB compared to other treatments. The combination therapy in the form of CyLiPn (CS-CyLiPn) showed significantly ($p < 0.05$) decreased levels compared to C-CyLiPn, S-CyLiPn and CS-Solution. The relative mRNA levels for TNFα and NF-κB were decreased by 1.74- and 1.86-folds in CS-CyLiPn compared to CS-Solution.

4. Discussion

The topical use of siRNA has been increasingly studied as a novel therapy for allergic skin diseases, which is attributed to its target-specific silencing effects [39]. RNAi offers potential for treating a wide variety of disorders through selective silencing of disease-relevant RNAs. Although direct injection of naked nucleic acids has been suggested as a possible delivery method [40], a large number of injections may be needed to achieve a therapeutic outcome. Among the numerous vehicles developed for siRNA delivery, cationic lipids and polymers can efficiently self-assemble with siRNA to form nano-complexes and have potential for delivering siRNA [41,42]. The ideal siRNA delivery system for the skin should have several characteristics: one to help siRNA to transverse the SC, second to protect siRNA during penetration process and third to facilitate siRNA uptake and efficient utilization by inflammatory cells. Several reports state that the siRNA can be used for anti-inflammatory therapy [39,43–45]. Our approach of targeting

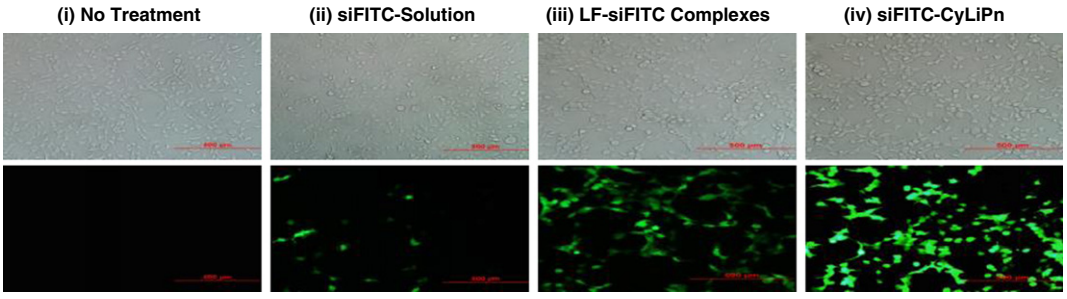

Fig. 4. Cellular uptake of siFITC in HEK-293 cells — microscopic images: fluorescent images of (i) no treatment (control) and cellular uptake of siFITC from (ii) siFITC-Solution, (iii) LF-siFITC complexes, (iv) siFITC-CyLiPn. Scale bars represent 500 µm. Here LF = Lipofectamine™ RNAiMAX.

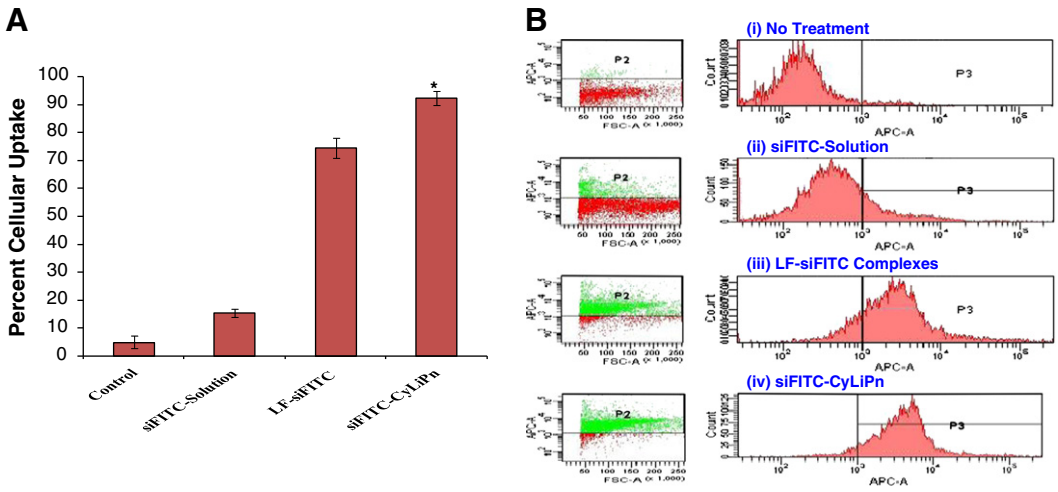

Fig. 5. Cellular uptake of siFITC in HEK-293 cells — FACS analysis: (A) Quantitative analysis of cellular uptake of siFITC using FACSCalibur. Data represent mean ± SD (n = 6); significance siFITC-CyLiPn against siFITC-solution and LF-siFITC complexes, *p < 0.05. (B) The flow cytometric picture of (i) non-treated (control) cells; and cells treated with (ii) siFITC-Solution, (iii) LF-siFITC complexes, (IV) siFITC-CyLiPn. Here LF = Lipofectamine™ RNAiMAX.

multiple factors such as simultaneous inhibition of neuropeptides while suppressing immune-response could be an efficient strategy to combat chronic inflammations. To fulfill these requirements in this study, we have developed a novel therapeutic approach for treating chronic inflammatory skin condition by utilizing siTNFα and Cap containing CyLiPns.

Use of cationic lipid in PLGA matrix has reported earlier for enhancing transfection properties of the resulting hybrid systems

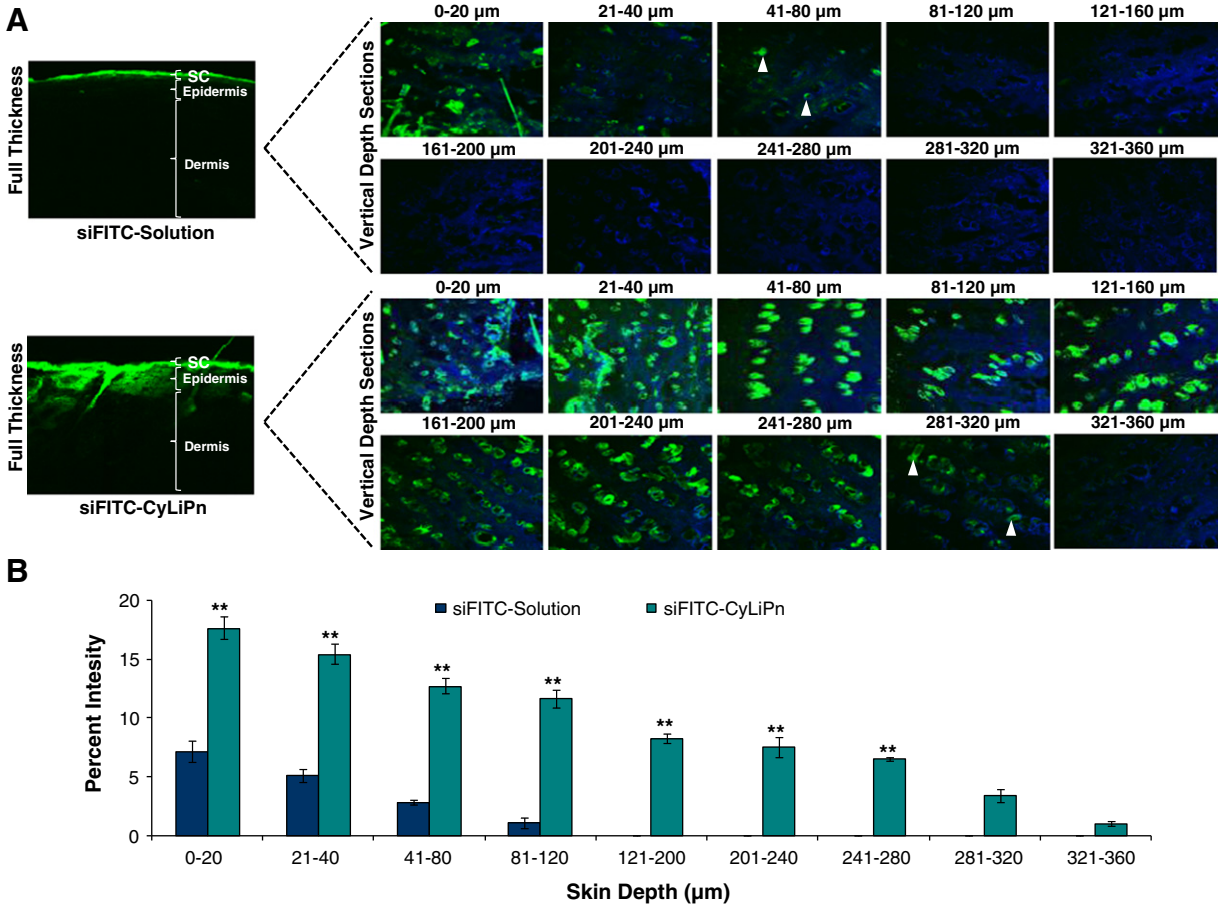

Fig. 6. CLSM images of lateral sections of siFITC permeated skin: After 24 h of *in vitro* rat skin permeation, skin was collected and lateral skin sections were observed under CLSM. (A) Lateral skin sections of different depths from 0 to 360 µm were observed for skin associated fluorescence. CyLiPn can deliver siFITC (bottom panel) up to 320 µm (white arrows). While, the siFITC-solution (naked siFITC, top panel) can penetrate only up to a skin depth of 80 µM (white arrows). The nuclei were stained by Hoechst (blue). (B) The percent fluorescence intensity of the siFITC-solution and siFITC–CyLiPn permeated skin sections were calculated from confocal images using digital image software. The percent intensity of the images was plotted against the skin depth for different CPPs. Data represent mean ± SD (n = 6); significance CyLiPn against solution, **p < 0.001.

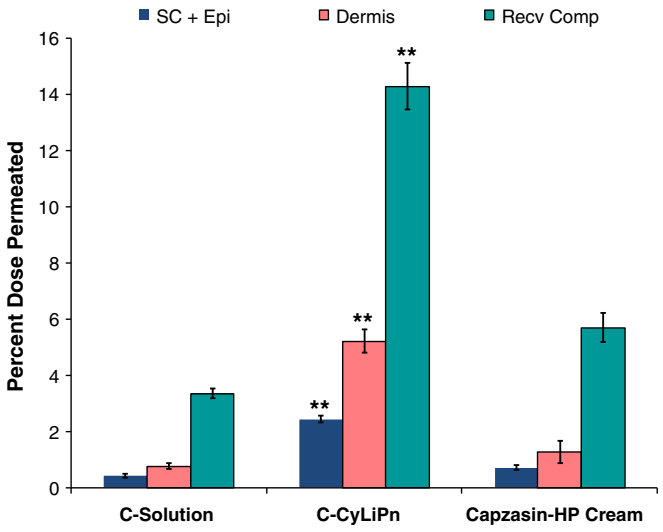

Fig. 7. *In vitro* skin permeation and distribution of Cap: the study was performed *in vitro* using Franz diffusion cells on rat skin for 24 h. The data represents %Dose permeated from different formulations of Cap. Data represent mean ± SD, n = 6; significance Cap-CyLiPn against C-solution and Capzasin-HP Cream, $^{**}p < 0.001$.

[32,46–49]. Here we have designed differentially charged core/shell lipid-polymer hybrid nanostructures (Fig. 1) that comprise three distinct components: (i) a negatively charged PLGA layer forming the inner core, where poorly water-soluble drug (Cap) was encapsulated; (ii) a lipid layer consisting of a novel, self penetrating, safe and cationic lipid synthesized with pyrrolidinium (cyclic) polar head group, which acts as a molecular fence to promote drug retention inside the polymeric core, thereby enhancing drug encapsulation efficiency and controlling drug release; and (iii) DSPE-PEG_{2000} forming outer layer. In CyLiPns, PLGA represents a model hydrophobic polymeric core to entrap Cap molecules; DSPE-PEG_{2000} was used as a hydrophilic polymer to form the stealth shell of nanoparticles and lipid monolayer consisting of a cationic lipid with cyclic pyrrolidinium head-group at the interface of the hydrophobic core and hydrophilic shell for delivering siRNA into deeper layers of the skin. CyLiPns showed a narrow size distribution (around 160 nm), as estimated by their low polydispersity index (PDI = 0.004). Zeta-potential measurements showed a positive surface charge of around 30 mV. This is due to the positive (+1) electrical charge on the quarternary ammonium in (N^+) pyrrolidinium head group of cationic lipid and is ideal for interaction with negatively charged nucleic acids, protecting the genetic material from degradation and enhancing the transfection efficiency.

Table 2
IMQ-induced skin inflammation in mice phenotypically resembles psoriasis. C57BL/6 mice were treated daily for 5 days with IMQ suspension on the shaved back skin and then the inflamed area was treated with CyLiPn formulations (C-CyLiPn, S-CyLiPn and CS-CyLiPn); CS-Solution; and Topgraf®. Psoriasis Area and Severity Index (PASI) score of the back skin was recorded daily on a scale from 0 to 4. Data represent mean ± SD (n = 6).

Day	Normal	IMQ	S-CyLiPn	C-CyLiPn	CS-CyLiPn	Topgraf®	C-Solution
1	0 ± 0	4 ± 0	4 ± 0	4 ± 0	4 ± 0	4 ± 0	4 ± 0
2	0 ± 0	4 ± 0	3 ± 0.55	3 ± 0.51	2 ± 0.55	1 ± 0.51	3 ± 0.41
3	0 ± 0	4 ± 0	2 ± 0.52	3 ± 0.41	2 ± 0.41	1 ± 0.41	3 ± 0.51
4	0 ± 0	4 ± 0	2 ± 0.52	3 ± 0.41	1 ± 0.51	0 ± 0.51	3 ± 0.51
5	0 ± 0	4 ± 0	2 ± 0.41	2 ± 0.55	0 ± 0.41	0 ± 0.41	3 ± 0.55

The most important aspect of the transdermal delivery is skin permeation. Heterocyclic compounds such as 6-aminohexanoates, azone and pyrrolidone derivatives such as (1-methyl-2-pyrrolidone, 1-ethyl-2-pyrrolidone, 1, 5-dimethyl-2-pyrrolidone, 5-methyl-2-pyrrolidone) are well studied chemical penetration enhancers [50]. However, their application is restricted due to higher toxicity profiles. In this study, we used a previously reported [24] cationic amphiphile with *3,4-dihydroxypyrrolidinium* as its hydrophilic polar head-group and two *stearyl fatty acyl chains* in its hydrophobic tail region. The findings of Chong-Kook Kim et al., suggested that the pyrrolidone derivatives incorporated into the lipid layer of the liposome increased the fluidity of the lipid layer in the liposome and such activity might have some correlation with the transdermal absorption-enhancing activity of therapeutics [51].

The present findings demonstrate that the nanoparticle containing cyclic-head lipid is capable to deliver siRNA and drug across deeper skin layers at levels required to produce a therapeutic effect. Although several important siRNA therapeutic targets in skin have been identified, the delivery of siRNA into skin has proved challenging. This limitation is potentially addressed through the studies reported here, since both PLGA and DSPE-PEG polymers have been approved by the Food and Drug Administration (FDA) for medical applications and cationic lipid used in this study has been found to be safe in pre-clinical studies [52]. Hence, we expect CyLiPns should be biocompatible, biodegradable and potentially safe as a drug carrier for clinical use. MTT-based cell viability assays in representative HEK293 cells revealed that CyLiPns are potentially non-cytotoxic. Percent cell viabilities were found to be remarkably high (>80%) when cells were treated with 20 μl of nanoparticles. The microscopic findings (Fig. 4) clearly demonstrate that the nanoparticle system is superior to commercially available siRNA transfection reagent Lipofectamine™ RNAiMAX. These findings were further confirmed with fluorescent-assisted cell sorting (FACS) analysis. Twenty percent more fluorescently-labeled cells were detected for CyLiPns treatment than Lipofectamine™ RNAiMAX (Fig. 5). The depth profiling of CyLiPn skin permeation showed that after 24 h, distinct fluorescence was observed up to a depth of 320 μm, which represents the deeper layers of the dermis. Further, in the lateral skin sections treated with naked siFITC solution, fluorescence was visible only in the appendages up to a depth of 40 μm. This is in agreement with previous reports where enhanced carboxyfluorescein-labeled siRNA delivery in rat skin was observed when coupled with cell penetrating peptide (TD-1) compared to naked siRNA [53]. Similarly, when the skin permeation experiment was performed using hairless rat skin, C-CyLiPn delivered 5.8, 2.9 and 4.2 folds more drugs than C-Solution and 3.5, 2.6 and 2.5 folds higher amounts of drug than marketed Capzasin-HP Cream in SC + Epi, dermis and receiver compartment, respectively. The enhanced permeation of Cap from CyLiPn may be the result of the combined effects of nanocarrier-mediated sustained release and cationic surface of the nanoparticles. Shah et al. [17] have also reported that when Ketoprofen and Spantide II were encapsulated in the PLGA-chitosan hybrid nanoparticles, skin retention of the drugs was increased significantly compared to when applied in a solution form due to strong affinity of positively charged amine groups (of chitosan) to the skin surface [17].

Psoriasis represents chronic inflammatory condition of the skin and during the inflammation various factors such as cytokines, chemokines and neuropeptides are altered. IMQ has been reported to induce skin inflammation in mice along with the features of human psoriasis where cytokines like IL-23 and IL-17 levels are elevated with typical phenotypic and histological characteristics [18,19]. Herein, we evaluated the efficacies of CyLiPns in psoriatic plaque-like inflammatory model. The enhanced anti-inflammatory responses of the combination treatment (CS-CyLiPn) in psoriatic plaque-like mouse model could be explained by the enhanced skin permeation of Cap with siTNFα. Cap is known to stimulate the

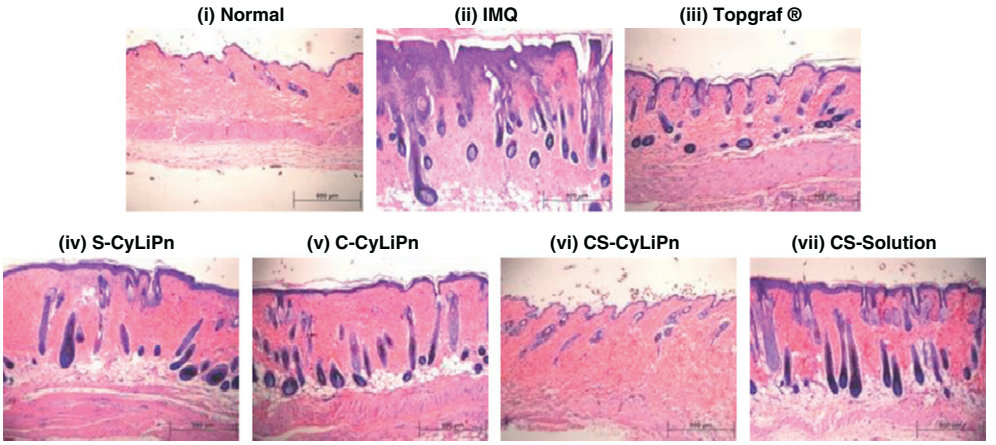

Fig. 8. H&E histological staining of: (i) normal skin, (ii) inflammation induced by topical application of IMQ suspension, and inflamed skin after 5 days of treatment with (iii) a positive control, Topgraf®, (iv) S-CyLiPn, (v) C-CyLiPn, (vi) CS-CyLiPn and (vii) CS-Solution. The decreased epidermal thickening with less infiltration of leukocytes was observed for CS-CyLiPn compared to C-CyLiPn, S-CyLiPn and CS-Solution. Scale bars represent 500 μm.

release of vasoactive neuropeptides such as substance P and calcitonin gene related peptide from C-fiber nerve terminal in the skin [54]. Park et al. demonstrated that Cap significantly inhibited the production of pro-inflammatory cytokine TNFα and also inhibited pro-inflammatory mediators through NF-κB, inactivation [55]. This suggests that Cap has a direct relation in altering the levels of TNFα and NF-κB. TNFα is a central regulator of inflammation, and it is well documented that TNFα is a potential therapeutic target in inflammatory diseases. Since elevated levels of TNFα plays a vital role in influencing several cytokines in the complex biology of inflammation, several TNFα antagonists such as infliximab, golimumab, adalimumab are in the market for treating inflammatory diseases [56,57]. The major concern of long-term treatment with these agents is the potential increase of infectious diseases or malignancy [58,59]. In addition, the cost of these biological agents is $20,000 to $30,000 per year per patient, which is a big hurdle for their extensive use in clinic. We anticipate that knockdown of TNFα would circumvent the disease condition with minimal side effects. Schiffers et al. demonstrated that direct intra-articular injection of TNF-α-specific siRNA to reduce joint inflammation in murine collagen-induced arthritis (CIA) and supported the use of siRNA-based therapies [29]. Furthermore, systemic delivery of TNFα specific siRNA using cationic

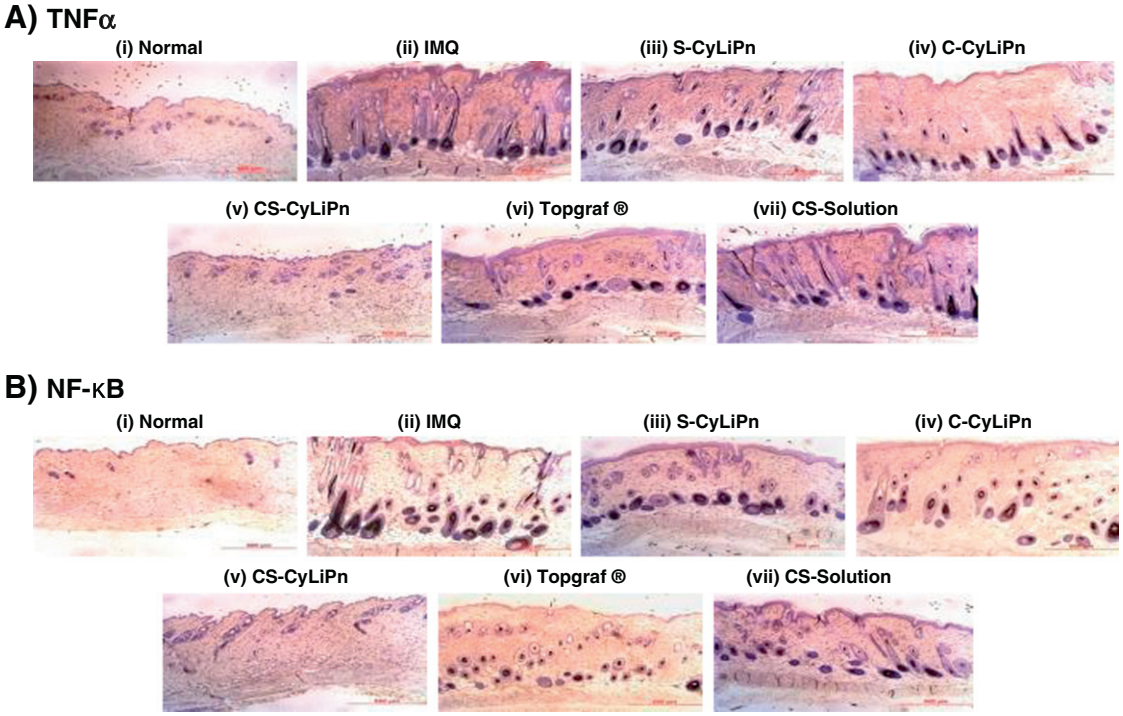

Fig. 9. Immunohistochemistry of (A) TNFα and (B) NF-κB for (i) normal skin, (ii) inflamed skin induced by topical application of IMQ suspension, and inflamed skin after 5 days of treatment with (iii) S-CyLiPn, (iv) C-CyLiPn, (v) CS-CyLiPn, (vi) a positive control, Topgraf® and (vii) CS-Solution. The presence of brown staining was considered a positive identification for activated TNFα or NF-κB. Scale bars represent 500 μm.

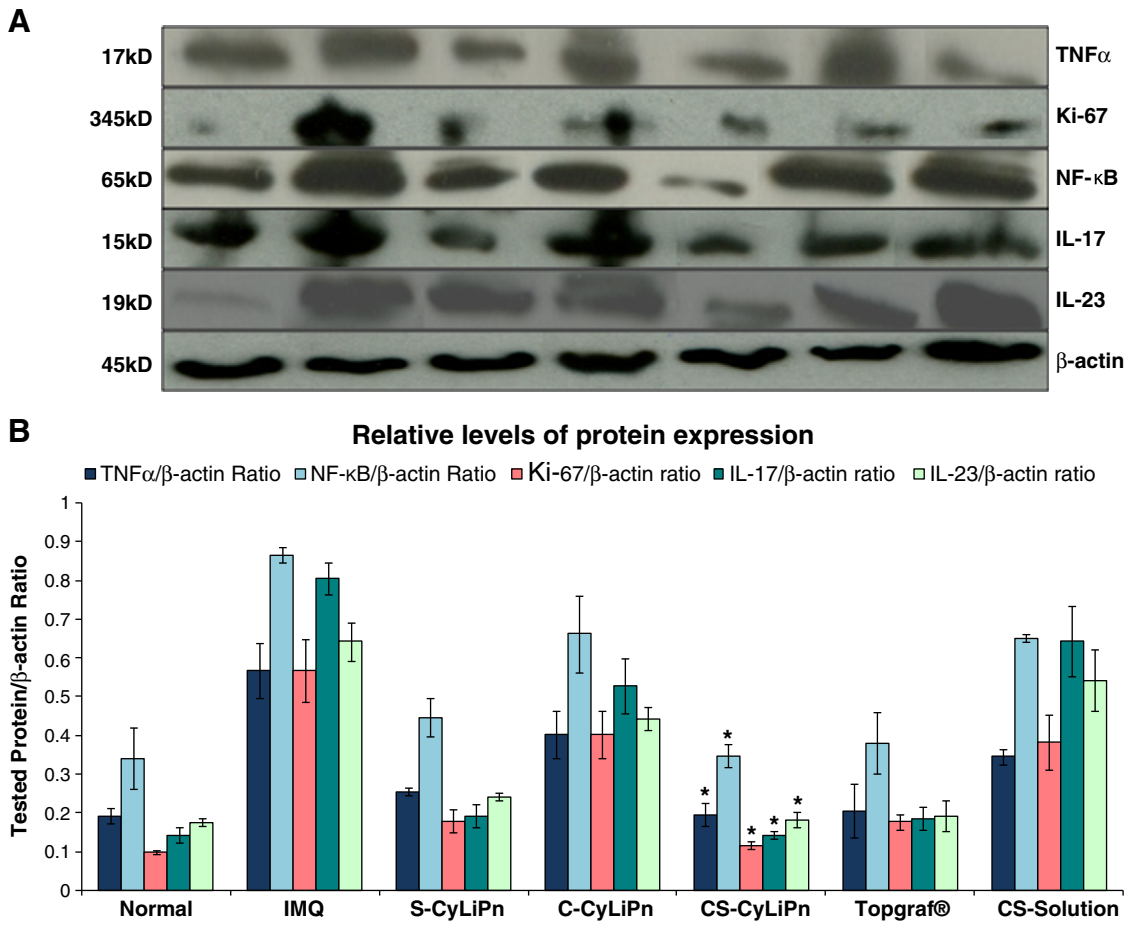

Fig. 10. Western blotting of skin lysates to determine (A) expression of inflammatory proteins in the skin and (B) quantification of inflammatory protein expressions (TNFα, Ki-67, NF-κB, IL-17 and IL-23) normalized by β-actin were investigated for normal skin, inflammation induced by topical application of IMQ suspension, and inflamed skin after 5 days of treatment with S-CyLiPn, C-CyLiPn, CS-CyLiPn, a positive control (Topgraf®) and CS-Solution. Data represent mean ± SD, n = 6; significance CS-CyLiPn against C-CyLiPn, S-CyLiPn, and CS-Solution, $^{*}p < 0.05$.

lipid-based nanoparticles shows effective anti-inflammatory effects in arthritic mice [30]. Importantly, both Cap and TNFα have independent mechanistic action, yet they have a common connection. Till date, no attempt has been made to target immune and neurocutaneous targets together to achieve therapeutic efficacy in treating inflammatory diseases and this is the most distinguishing aspect of the present study.

The calculated combination index value suggested moderate synergism for CyLiPns over the entire study period which might be because of two different mechanisms of Cap and siTNFα working together in reducing the cutaneous inflammation. The epidermal thickening, elongation of epidermal rete ridges, infiltration of leukocytes, IL-23 and IL-17 levels were significantly less ($p < 0.05$) in CS-CyLiPn compared to C-CyLiPn, S-CyLiPn and control, signifying the effectiveness of CS-CyLiPn. Tacrollimus is a topically applied immunosuppressant, to reduce psoriatic plaque inflammations [19,20]. Previous studies including our own, demonstrated that commercially available formulation of tacrolimus, Topgraf® exhibited superior activity than several other formulations [19,20]. Interestingly, CS-CyLiPn nanoparticle system was equally comparable with Topgraf®. The levels of inflammatory protein, TNFα, Ki-67, NF-κB, IL-17 and IL-23 were significantly less ($p < 0.05$) in CS-CyLiPn compared with either of the drugs alone and more interestingly the levels of these proteins were slightly lesser than Topgraf®. Collectively, our results suggest that topical Cap + siTNFα treatment downregulates the TNFα and NF-κB functions quantitatively and qualitatively *in vivo*. From the current study it can be assumed that the enhanced penetration of both intact nanoparticles and the released siTNFα and/or Cap molecules is a result of active interaction between SC components (corneocytes and lipids) and novel cyclic lipid of CyLiPn. On application of CyLiPn on the skin surface, the following sequence of events may take place: (i) ionic interaction between positively charged outer lipid layer of CyLiPn with negatively charged residues of the proteins and lipids of SC; (ii) beyond a threshold concentration of CyLiPn, a transitional destabilization of the membrane may occur; (iii) hybrid nanoparticles form a film over the skin surface leading to higher hydrating effects resulting in SC swelling and opening allows subsequent higher penetration of permeant; (iv) finally, CyLiPn and encapsulated substances may penetrate through hair follicles and furrows where they can act as a drug reservoirs.

5. Conclusion

Toward treating chronic skin inflammations, we have designed a novel carrier system for delivering anti-inflammatory agents siTNFα and Cap into deep dermal milieu. Our studies demonstrate that nanoparticle system coated with cationic lipid with cyclic pyrrolidinium head group enhanced skin permeation of fluorescently-labeled

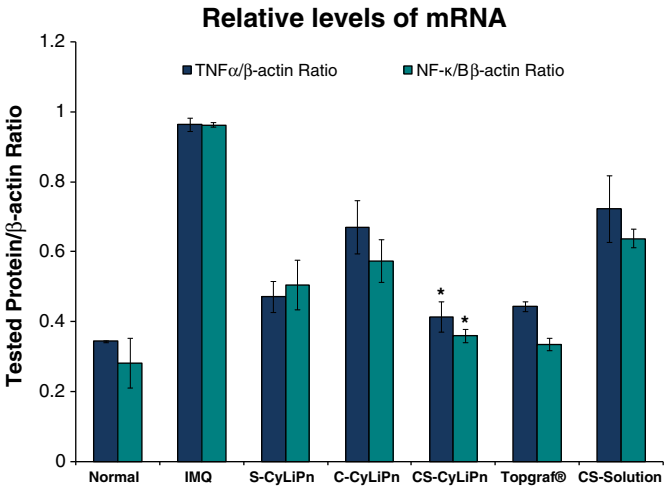

Fig. 11. Relative mRNA expression levels by RT-PCR: Real-time PCR was performed and the mRNA expression levels of TNFα and NF-κB normalized by β-actin were investigated for normal skin, inflammation induced by topical application of IMQ suspension, and inflamed skin after 5 days of treatment with S-CyLiPn, C-CyLiPn, CS-CyLiPn, a positive control (Topgraf®) and CS-Solution. Data represent mean ± SD, n = 6; significance CS-CyLiPn against C-CyLiPn, S-CyLiPn, and CS-Solution, $^{*}p < 0.05$.

siRNA containing nanoparticles. Efficacies of these nanoparticles were evaluated in psoriatic plaque-like mouse model which represents chronic skin inflammations. Findings in PASI Index, Western blot analysis of various inflammatory markers and quantification of mRNA levels of TNFα and NF-κB upon the treatment of nanoparticles with their control groups, taken together, support the notion that siTNFα and Cap show synergism in treating inflammatory skin disorders like psoriasis. In summary, the present findings demonstrate for the first time that cationic lipid-polymer hybrid nanoparticles can efficiently carry siTNFα and Cap into the deeper dermal milieu.

Acknowledgements

We thank Dr. Punit P. Shah, College of Pharmacy and Pharmaceutical Sciences, Florida A&M University, Tallahassee, FL 32307, USA for his kind help in developing psoriatic plaque-like mouse model. This project was supported by the National Center for Research Resources and the National Institute of Minority Health and Health Disparities of the National Institutes of Health through Grant Number 8 G12 MD007582-28 and 2 G12 RR003020.

Appendix A. Supplementary data

Supplementary data to this article can be found online at http://dx.doi.org/10.1016/j.jconrel.2013.04.021.

References

[1] R.N. Herrier, Advances in the treatment of moderate-to-severe plaque psoriasis, Am. J. Health Syst. Pharm. 68 (2011) 795–806.
[2] C.E. Griffiths, B.E. Strober, P. van de Kerkhof, V. Ho, R. Fidelus-Gort, N. Yeilding, C. Guzzo, Y. Xia, B. Zhou, S. Li, L.T. Dooley, N.H. Goldstein, A. Menter, Comparison of ustekinumab and etanercept for moderate-to-severe psoriasis, N. Engl. J. Med. 362 (2010) 118–128.
[3] W. Hueber, D.D. Patel, T. Dryja, A.M. Wright, I. Koroleva, G. Bruin, C. Antoni, Z. Draelos, M.H. Gold, P. Durez, P.P. Tak, J.J. Gomez-Reino, C.S. Foster, R.Y. Kim, C.M. Samson, N.S. Falk, D.S. Chu, D. Callanan, Q.D. Nguyen, K. Rose, A. Haider, F. Di Padova, Effects of AIN457, a fully human antibody to interleukin-17A, on psoriasis, rheumatoid arthritis, and uveitis, Sci. Transl. Med 2 (2010) 52ra72.
[4] M.A. Lowes, A.M. Bowcock, J.G. Krueger, Pathogenesis and therapy of psoriasis, Nature 445 (2007) 866–873.
[5] S. Kawai, H. Sekino, N. Yamashita, S. Tsuchiwata, H. Liu, J.M. Korth-Bradley, The comparability of etanercept pharmacokinetics in healthy Japanese and American subjects, J. Clin. Pharmacol. 46 (2006) 418–423.
[6] S.M. Elbashir, J. Harborth, W. Lendeckel, A. Yalcin, K. Weber, T. Tuschl, Duplexes of 21-nucleotide RNAs mediate RNA interference in cultured mammalian cells, Nature 411 (2001) 494–498.
[7] E.R. Rayburn, R. Zhang, Antisense, RNAi, and gene silencing strategies for therapy: mission possible or impossible? Drug Discov. Today 13 (2008) 513–521.
[8] B. Geusens, N. Sanders, T. Prow, M. Van Gele, J. Lambert, Cutaneous short-interfering RNA therapy, Expert Opin. Drug Deliv. 6 (2009) 1333–1349.
[9] K. Moser, K. Kriwet, A. Naik, Y.N. Kalia, R.H. Guy, Passive skin penetration enhancement and its quantification *in vitro*, Eur. J. Pharm. Biopharm. 52 (2001) 103–112.
[10] B.W. Barry, Novel mechanisms and devices to enable successful transdermal drug delivery, Eur. J. Pharm. Sci. 14 (2001) 101–114.
[11] N. Kanikkannan, K. Kandimalla, S.S. Lamba, M. Singh, Structure–activity relationship of chemical penetration enhancers in transdermal drug delivery, Curr. Med. Chem. 7 (2000) 593–608.
[12] S. Rawat, S. Vengurlekar, B. Rakesh, S. Jain, G. Srikarti, Transdermal delivery by iontophoresis, Indian J. Pharm. Sci. 70 (2008) 5–10.
[13] B. Ferraro, L.C. Heller, Y.L. Cruz, S. Guo, A. Donate, R. Heller, Evaluation of delivery conditions for cutaneous plasmid electrotransfer using a multielectrode array, Gene Ther. 18 (2011) 496–500.
[14] B.E. Polat, D. Hart, R. Langer, D. Blankschtein, Ultrasound-mediated transdermal drug delivery: mechanisms, scope, and emerging trends, J. Control. Release 152 (2011) 330–348.
[15] R.R. Patlolla, P.R. Desai, K. Belay, M.S. Singh, Translocation of cell penetrating peptide engrafted nanoparticles across skin layers, Biomaterials 31 (2010) 5598–5607.
[16] P.R. Desai, P.P. Shah, R.R. Patlolla, M. Singh, Dermal microdialysis technique to evaluate the trafficking of surface-modified lipid nanoparticles upon topical application, Pharm. Res. 29 (2012) 2587–2600.
[17] P.P. Shah, P.R. Desai, M. Singh, Effect of oleic acid modified polymeric bilayered nanoparticles on percutaneous delivery of spantide II and ketoprofen, J. Control. Release 158 (2012) 336–345.
[18] P.P. Shah, P.R. Desai, A.R. Patel, M.S. Singh, Skin permeating nanogel for the cutaneous co-delivery of two anti-inflammatory drugs, Biomaterials 33 (2012) 1607–1617.
[19] P.P. Shah, P.R. Desai, D. Channer, M. Singh, Enhanced skin permeation using polyarginine modified nanostructured lipid carriers, J. Control. Release 161 (2012) 735–745.
[20] P. Desai, R.R. Patlolla, M. Singh, Interaction of nanoparticles and cell-penetrating peptides with skin for transdermal drug delivery, Mol. Membr. Biol. 27 (2010) 247–259.
[21] B.K. Majeti, P.P. Karmali, B.S. Reddy, A. Chaudhuri, *In vitro* gene transfer efficacies of N, N-dialkylpyrrolidinium chlorides: a structure–activity investigation, J. Med. Chem. 48 (2005) 3784–3795.
[22] P.W. Lee, S.H. Hsu, J.S. Tsai, F.R. Chen, P.J. Huang, C.J. Ke, Z.X. Liao, C.W. Hsiao, H.J. Lin, H.W. Sung, Multifunctional core–shell polymeric nanoparticles for transdermal DNA delivery and epidermal Langerhans cells tracking, Biomaterials 31 (2010) 2425–2434.
[23] P.P. Karmali, A. Chaudhuri, Cationic liposomes as non-viral carriers of gene medicines: resolved issues, open questions, and future promises, Med. Res. Rev. 27 (2007) 696–722.
[24] B.K. Majeti, R.S. Singh, S.K. Yadav, S.R. Bathula, S. Ramakrishna, P.V. Diwan, S.S. Madhavendra, A. Chaudhuri, Enhanced intravenous transgene expression in mouse lung using cyclic-head cationic lipids, Chem. Biol. 11 (2004) 427–437.
[25] M.M. Janat-Amsbury, J.W. Yockman, M. Lee, S. Kern, D.Y. Furgeson, M. Bikram, S.W. Kim, Combination of local, nonviral IL12 gene therapy and systemic paclitaxel treatment in a metastatic breast cancer model, Mol. Ther. 9 (2004) 829–836.
[26] Y. Wang, S. Gao, W.H. Ye, H.S. Yoon, Y.Y. Yang, Co-delivery of drugs and DNA from cationic core–shell nanoparticles self-assembled from a biodegradable copolymer, Nat. Mater. 5 (2006) 791–796.
[27] R.W. Malone, M.A. Hickman, K. Lehmann-Bruinsma, T.R. Sih, R. Walzem, D.M. Carlson, J.S. Powell, Dexamethasone enhancement of gene expression after direct hepatic DNA injection, J. Biol. Chem. 269 (1994) 29903–29907.
[28] C.S. Kim, T. Kawada, B.S. Kim, I.S. Han, S.Y. Choe, T. Kurata, R. Yu, Capsaicin exhibits anti-inflammatory property by inhibiting IκB-a degradation in LPS-stimulated peritoneal macrophages, Cell. Signal. 15 (2003) 299–306.
[29] R.M. Schiffelers, J. Xu, G. Storm, M.C. Woodle, P.V. Scaria, Effects of treatment with small interfering RNA on joint inflammation in mice with collagen-induced arthritis, Arthritis Rheum. 52 (2005) 1314–1318.
[30] M. Khoury, P. Louis-Plence, V. Escriou, D. Noel, C. Largeau, C. Cantos, D. Scherman, C. Jorgensen, F. Apparailly, Efficient new cationic liposome formulation for systemic delivery of small interfering RNA silencing tumor necrosis factor alpha in experimental arthritis, Arthritis Rheum. 54 (2006) 1867–1877.
[31] K.A. Howard, S.R. Paludan, M.A. Behlke, F. Besenbacher, B. Deleuran, J. Kjems, Chitosan/siRNA nanoparticle-mediated TNF-alpha knockdown in peritoneal macrophages for anti-inflammatory treatment in a murine arthritis model, Mol. Ther. 17 (2009) 162–168.
[32] L. Zhang, J.M. Chan, F.X. Gu, J.W. Rhee, A.Z. Wang, A.F. Radovic-Moreno, F. Alexis, R. Langer, O.C. Farokhzad, Self-assembled lipid-polymer hybrid nanoparticles: a robust drug delivery platform, ACS Nano 2 (2008) 1696–1702.
[33] T. Lobovkina, G.B. Jacobson, E. Gonzalez-Gonzalez, R.P. Hickerson, D. Leake, R.L. Kaspar, C.H. Contag, R.N. Zare, *In vivo* sustained release of siRNA from solid lipid nanoparticles, ACS Nano 5 (2011) 9977–9983.
[34] J. Du, Y. Sun, Q.S. Shi, P.F. Liu, M.J. Zhu, C.H. Wang, L.F. Du, Y.R. Duan, Biodegradable nanoparticles of mPEG-PLGA-PLL triblock copolymers as novel non-viral

vectors for improving siRNA delivery and gene silencing, Int. J. Mol. Sci. 13 (2012) 516–533.
[35] R.J. Babu, N. Kanikkannan, L. Kikwai, C. Ortega, S. Andega, K. Ball, S. Yim, M. Singh, The influence of various methods of cold storage of skin on the permeation of melatonin and nimesulide, J. Control. Release. 86 (2003) 49–57.
[36] J.N. Kearney, Guidelines on processing and clinical use of skin allografts, Clin. Dermatol. 23 (2005) 357–364.
[37] Y.Y. Wang, C.T. Hong, W.T. Chiu, J.Y. Fang, *In vitro* and *in vivo* evaluations of topically applied capsaicin and nonivamide from hydrogels, Int. J. Pharm. 224 (2001) 89–104.
[38] L. van der Fits, S. Mourits, J.S. Voerman, M. Kant, L. Boon, J.D. Laman, F. Cornelissen, A.M. Mus, E. Florencia, E.P. Prens, E. Lubberts, Imiquimod-induced psoriasis-like skin inflammation in mice is mediated *via* the IL-23/IL-17 axis, J. Immunol. 182 (2009) 5836–5845.
[39] M.B. Chougule, A.R. Patel, T. Jackson, M. Singh, Antitumor activity of Noscapine in combination with Doxorubicin in triple negative breast cancer, PLoS One 6 (2011) e17733.
[40] N. Ichite, M. Chougule, A.R. Patel, T. Jackson, S. Safe, M. Singh, Inhalation delivery of a novel diindolylmethane derivative for the treatment of lung cancer, Mol. Cancer Ther. 9 (2010) 3003–3014.
[41] T. Uchida, T. Kanazawa, M. Kawai, Y. Takashima, H. Okada, Therapeutic effects on atopic dermatitis by anti-RelA short interfering RNA combined with functional peptides Tat and AT1002, J. Pharmacol. Exp. Ther. 338 (2011) 443–450.
[42] U.R. Hengge, P.S. Walker, J.C. Vogel, Expression of naked DNA in human, pig, and mouse skin, J. Clin. Invest. 97 (1996) 2911–2916.
[43] Y.C. Tseng, S. Mozumdar, L. Huang, Lipid-based systemic delivery of siRNA, Adv. Drug Deliv. Rev. 61 (2009) 721–731.
[44] K.A. Howard, Delivery of RNA interference therapeutics using polycation-based nanoparticles, Adv. Drug Deliv. Rev. 61 (2009) 710–720.
[45] P. Ritprajak, M. Hashiguchi, M. Azuma, Topical application of cream-emulsified CD86 siRNA ameliorates allergic skin disease by targeting cutaneous dendritic cells, Mol. Ther. 16 (2008) 1323–1330.
[46] J.Y. Kim, J.Y. Shin, M.R. Kim, S.K. Hann, S.H. Oh, siRNA-mediated knock-down of COX-2 in melanocytes suppresses melanogenesis, Exp. Dermatol. 21 (2012) 420–425.
[47] D. Zheng, D.A. Giljohann, D.L. Chen, M.D. Massich, X.Q. Wang, H. Iordanov, C.A. Mirkin, A.S. Paller, Topical delivery of siRNA-based spherical nucleic acid nanoparticle conjugates for gene regulation, Proc. Natl. Acad. Sci. U.S.A. 109 (2012) 11975–11980.
[48] S. Diez, I. Migueliz, C. Tros de Ilarduya, Targeted cationic poly(D, L-lactic-co-glycolic acid) nanoparticles for gene delivery to cultured cells, Cell. Mol. Biol. Lett. 14 (2009) 347–362.
[49] S. Diez, G. Navarro, G. Navarro, I.C.T. de, *In vivo* targeted gene delivery by cationic nanoparticles for treatment of hepatocellular carcinoma, J. Gene Med. 11 (2009) 38–45.
[50] D.K. Jensen, L.B. Jensen, S. Koocheki, L. Bengtson, D. Cun, H.M. Nielsen, C. Foged, Design of an inhalable dry powder formulation of DOTAP-modified PLGA nanoparticles loaded with siRNA, J. Control. Release 157 (2012) 141–148.
[51] J. Shi, Z. Xiao, A.R. Votruba, C. Vilos, O.C. Farokhzad, Differentially charged hollow core/shell lipid-polymer-lipid hybrid nanoparticles for small interfering RNA delivery, Angew. Chem. Int. Ed. Engl. 50 (2011) 7027–7031.
[52] A.C. Williams, B.W. Barry, Penetration enhancers, Adv. Drug Deliv. Rev. 56 (2004) 603–618.
[53] C.-K. Kim, M.-S. Hong, Y.-B. Kim, S.-K. Han, Effect of penetration enhancers (pyrrolidone derivatives) on multilamellar liposomes of stratum corneum lipid: a study by UV spectroscopy and differential scanning calorimetry, Int. J. Pharm. 95 (1993) 43–50.
[54] M. Lopez-Cervantes, E. Marquez-Mejia, J. Cazares-Delgadillo, D. Quintanar-Guerrero, A. Ganem-Quintanar, E. Angeles-Anguiano, Chemical enhancers for the absorption of substances through the skin: laurocapram and its derivatives, Drug Dev. Ind. Pharm. 32 (2006) 267–286.
[55] K.R. Pawar, R.J. Babu, Polymeric and lipid-based materials for topical nanoparticle delivery systems, Crit. Rev. Ther. Drug Carrier Syst. 27 (2010) 419–459.
[56] C.M. Lin, K. Huang, Y. Zeng, X.C. Chen, S. Wang, Y. Li, A simple, noninvasive and efficient method for transdermal delivery of siRNA, Arch. Dermatol. Res. 304 (2012) 139–144.
[57] L. Tavano, P. Alfano, R. Muzzalupo, B. de Cindio, Niosomes vs microemulsions: new carriers for topical delivery of Capsaicin, Colloids Surf. B Biointerfaces 87 (2011) 333–339.
[58] J.Y. Park, T. Kawada, I.S. Han, B.S. Kim, T. Goto, N. Takahashi, T. Fushiki, T. Kurata, R. Yu, Capsaicin inhibits the production of tumor necrosis factor alpha by LPS-stimulated murine macrophages, RAW 264.7: a PPARgamma ligand-like action as a novel mechanism, FEBS Lett. 572 (2004) 266–270.
[59] G.E. Pierard, C. Pierard-Franchimont, G. Szepetiuk, P. Paquet, P. Quatresooz, The therapeutic potential of TNF-alpha antagonists for skin psoriasis comorbidities, Expert. Opin. Biol. Ther. 10 (2010) 1197–1208.